Immersed interlaminar fatigue of glass fiber epoxy composites using the I-beam method

Abedin I. Gagani, Emeric P.V. Mialon, Andreas T. Echtermeyer

PII: S0142-1123(18)30363-3
DOI: https://doi.org/10.1016/j.ijfatigue.2018.10.011
Reference: JIJF 4875

To appear in: *International Journal of Fatigue*

Received Date: 14 August 2018
Revised Date: 10 October 2018
Accepted Date: 12 October 2018

Please cite this article as: Gagani, A.I., Mialon, E.P.V., Echtermeyer, A.T., Immersed interlaminar fatigue of glass fiber epoxy composites using the I-beam method, *International Journal of Fatigue* (2018), doi: https://doi.org/10.1016/j.ijfatigue.2018.10.011

Immersed interlaminar fatigue of glass fiber epoxy composites using the I-beam method

Abedin I. Gagani, Emeric P.V. Mialon, Andreas T. Echtermeyer

Department of Mechanical and Industrial Engineering, Norwegian University of Science and Technology (NTNU), Trondheim, Norway

Corresponding author: abedin.gagani@ntnu.no +47 7359 3885

Abstract

Exposure to marine environment causes a degradation of the interlaminar shear performance of composites. This effect has been reported in several studies, but the mechanisms that lead to failure in composites subjected to cyclic loading under water exposure are still not fully understood. In this work a novel test method, the I-beam short beam shear, was used to determine shear properties and accelerate fluid saturation in glass fiber epoxy specimens. The interlaminar shear performance of the material was studied experimentally. From the analysis of the cyclic parameters recorded during the test and from optical micrographs it was possible to observe a change in failure mode between dry samples and conditioned samples. The failure of dry samples was a creep dominated effect, which led to inter-ply cracks, while the failure of conditioned samples was a damage growth dominated effect, which led to intra-ply failure. Optical micrographs showed that fiber/matrix debonding occurs in conditioned samples prior to mechanical loading, which are potential damage onset spots.

Keywords: Composites; Cyclic properties; Durability; Environmental assisted fatigue; Environmental effects.

1. Introduction

Composites have a wide potential to be used in offshore applications. They combine light weight, good fatigue characteristics and can be built easily in complicated shapes. However, composites show some degradation of properties when exposed to water, especially at high temperatures. This degradation needs to be understood and considered in design, because offshore structures operate under these conditions. In particular, cyclic loading combined with water degradation can lead to an accelerated final failure of the composite [1, 2].

Composite components are frequently connected to components made of other materials, typically metals. High interlaminar shear stresses tend to be present at connections, making the interlaminar shear strength a critical design parameter. This paper investigates the degradation of interlaminar shear fatigue strength due to hygrothermal aging.

For wind turbine blades [3] and offshore composite structures like pipes [4], design life is long (up to 50 years for offshore pipes) and durability must be ensured until the last day of service life [5]. Testing of a real composite structure under realistic operational conditions is often not possible, as it would require years to reach fluid saturation and to finally test the structure. A better approach to obtain long term performance of a large structure is to test and understand properties on the material level. The performance of the component can then be calculated [6].

Many methods are available for interlaminar shear testing of marine composites on the material level, like three-point bending, four-point bending, Iopescu and more [7]. Interlaminar shear properties are not necessarily the same as in-plane shear properties,

especially for thermoplastic materials. It is however hard to find a test method that allows quick saturation of the sample, due to the typically high thickness of the sample. Fickian diffusion theory suggests that the time needed to reach saturation is proportional to the square of the thickness of the specimen. One of the most popular method for testing interlaminar shear is Short Beam Shear (SBS) testing. The absolute shear strength obtained from SBS samples is often questioned, since the shear stress field is not uniform along the length and thickness of the sample, as discussed in the ASTM D2344 Standard [8], but they give a good indication of the relative change of properties. For this reason, the test is often used for production control. But the test is also useful for investigating the change of properties due to environmental effects [9]. The SBS samples with a rectangular cross section suffer still from long saturation times when exposed to water. Thin samples would therefore be beneficial, but they suffer from several problems especially indentation under the loading-pin. A new I-beam shaped test sample was used here that provides the simplicity of testing SBS samples in bending. These samples have the advantage of requiring only few weeks to reach saturation at elevated temperature and yet reduce loading pin indentation due to the presence of wider top and bottom flanges. Based on Fickian diffusion theory a thickness reduction from 4 to 2 mm enables reaching saturation four times faster. The disadvantage of this sample geometry is the more complicated shape, compared to regular SBS. The sample geometry is shown in **Fig. 1** and dimensions are reported in **Table 1**.

Fig. 1 (a) Geometry and dimensions of tested I-beams, (b) four-point bending test setup and dimensions

Table 1 Dimensions of the I-beam specimen

In the present work dry short I-beam shaped samples were tested in four point bending in air and compared to the results of samples conditioned and tested in water.

Mechanical parameters, like dynamic secant modulus, dissipated energy per loading cycle and minimum cyclic deflection, were recorded during the test. They were later analysed, in order to get an insight about the failure mechanisms for dry and conditioned samples. Optical microscope analyses were performed on tested samples and on untested samples after conditioning, in order to investigate the presence of hygrothermal induced damage.

2. Material and methods

2.1. Materials

A 32-plies unidirectional glass fiber/epoxy composite laminate was manufactured using vacuum assisted resin transfer molding (VARTM). The matrix was Hexion Epikote^{TM} Resin RIMR135 mixed with Epikure^{TM} Curing Agent MGS RIMH137 with a mixing ratio of 100:30 by weight. The fibers were HiPer-tex UD glass fibers from 3B. Curing was performed at room temperature for 24h and post-curing in a ventilated oven at 80˚C for 16 h. The fiber volume fraction of the laminate was obtained by matrix burnoff test [10], resulting in 60.1 %. I-beam shaped samples were obtained by first cutting a laminate with a diamond coated saw into rectangular bars, which were then milled to the geometry shown in **Fig. 1**. Samples were cut into the final length with a circular water-cooled diamond coated saw. Sample edges were ground up to 4000 grit and polished to 1 μm, in order to reduce potential stress concentrations.

The samples were dried in a ventilated oven for 72 hours at 60 °C and a set of samples was immersed in distilled water at 60 ± 1 °C until saturation occurred, according to ASTM D5229 Standard [11].

Dynamic thermal mechanical analysis was performed on dry and conditioned tensile samples using a Netzsch-Gabo Eplexor 150 DMTA machine equipped with a 150 N load cell and a thermal chamber, resulting in glass transition temperature, T_g = 87.1°C for dry samples and

T_g = 49.0°C for conditioned samples [12]. The conditioning temperature of 60 °C was chosen to accelerate fluid saturation, being more than 25 °C below the T_g of the dry material, according to the recommendation in the standard [11]. The decrease of T_g of the saturated samples below the conditioning temperature implies a reversible change in mechanical properties of the material at the conditioning temperature. However, it is important to remark that the mechanical properties of the material at room temperature are believed to be not influenced by this effect, since full curing of the resin was reached during the curing and post-curing processes performed after resin infusion in the laminate, so no additional cross-links were created during conditioning.

2.2. Interlaminar shear fatigue testing

Four point bending testing was performed on the I-beam short beam shear configuration (ISBS) shown in Figure 1, using an Instron 1342 servo hydraulic testing machine with a 50 kN loadcell. The test was performed in load control, with a ratio R = 0.1 and a frequency of 4 Hz, in order to reduce the effect of heat generated by loading. For samples that reached 2 000 000 cycles, the test was stopped and the result were defined as a run-out. The setup used for the immersed tests is shown in **Fig. 2 (a)**. A polycarbonate (PC) antibuckling device was used in order to avoid buckling of the sample´s central web, as shown schematically in **Fig. 2 (b)** [12].

Failure was defined when the samples reached a limit deflection equal to the static deflection at failure for that test environment (dry or conditioned). In **Fig. 2 (c)** are reported other possible definitions of failure for a SBS test, like the knee of the deflection curve or the limit of the set-up, when further deflection would damage the set-up. The static deflection at failure was chosen since it is the most reproducible criterion. It was verified that the choice of

the failure criterion has little influence for the material studied here. When dealing with different materials it is recommended to verify the validity of this assumption.

Fig. 2 (a) Testing set-up for I-beam short beam shear test, (b) polycarbonate antibuckling device: front and top view, (c) schematic evolution of maximum cyclic deflection.

An additional control was performed by testing twelve SBS samples of the same material having the conventional rectangular geometry with dimensions according to the ASTM D2344 standard for short beam shear testing: 7 x 14 x 42 mm [8]. The span length adopted was 28 mm and the loading pins diameters were 6 mm for the top and 3 mm for the bottom, according to the standard [8]. The SBS samples have been tested only in dry state and not in saturated state, due to the long time required to reach saturation compared to the I-beam samples. The SBS samples are 3.5 times thicker than the I-beam samples, and would require 12.25 longer time to reach saturation, according to Fickian diffusion theory.

3. Results

3.1. Weight gain curve

Conditioning was concluded when the samples reached saturation, which was defined when the mass increase between two consecutive measurements was below 0.02 %, according to the ASTM D5229 standard [11]. The results of the mass increase measurements are reported in **Fig. 3**. The moisture saturation content was 0.78 % ± 0.01%, which is very close to the theoretical value predicted for the same matrix material and fibre properties using micromechanical theory in [13]: 0.774%.

Fig. 3. Average weight gain curves. Each point is the average of 13 samples.

It can be noticed that a small drop or plateau is visible in **Fig.3** between 12^2 and 18^2 hours. This drop could be attributed to the saturation of the central web of the I-beam while the flange has not reached complete saturation.

3.2. SN curves

The SN curves are shown in **Fig. 4**, and were analysed using Basquin relation, **Fig. 4 (a)** [14]:

$$L = L_0 N^{-1/k} \quad (1)$$

where L is the load, L_0 the pre-exponential load coefficient, N the number of cycles and k the slope. The fatigue laws obtained using Eq. (1) were 10.91 $N^{-1/18.6}$ for dry samples and 7.58 $N^{-14.1}$ for conditioned samples, **Fig.4**, indicating a potential change of the failure mode. It is interesting to notice that the values of L_0 for both dry and conditioned samples are close to the static loads to failure, which were 9.6 and 6.55 kN respectively [12].

In **Fig. 4 (b)** the same results were plotted in a linear load scale and analysed using the following equation:

$$L = L_0 - N^{-1/k} \quad (2)$$

Fig. 4. S-N curves of dry samples tested in air and previously saturated samples tested in immersion. (a) Regression performed according to Basquin relation, Eq. (1). (b) Regression is performed according to Eq. (2).

From **Figs. 4 (a-b)** it can be noted that with increasing number of cycles, the dry and conditioned SN curves seem to converge in a linear-log scale, **Fig. 4 (a)**, and seem to diverge in a log-log scale, **Fig. 4 (b)**. A similar effect but less severe can be seen for the results published in [9].

When testing traditional rectangular beams, the through thickness shear strength can be calculated according to simple analytical formulas that are also given in the ASTM and ISO standards. There is some controversy about the applicability of the formulas for nonlinear and anisotropic materials [15, 16]. Obtaining the absolute value of the shear strength gets even

more complicated for the I-beam specimen [9]. This paper does not address this issue, but simply uses the test results for comparing dry and wet fatigue properties.

The traditional short beam shear testing and the I-beam method allow quick evaluation of the relative change in strength between dry and conditioned samples. This is shown by comparing the experimental SN curves obtained in this study with published results for a similar material [9] and with tests performed on samples made of the same material using the standard ASTM D2344 geometry [8]. The results yield a good agreement, as shown in **Fig. 5**, confirming the accuracy of the I-beam short beam shear method in capturing environmental degradation, compared with the standard methods, while strongly reducing the time required for conditioning.

Fig. 5. Normalized S-N curves. The results are compared to the ones reported by Rocha *et al.* [9] and to the set of standard SBS samples tested. The fit lines are based only on the I-beam data, as shown in Fig.4 (a).

3.3.Effect of creep and damage

The interlaminar shear behaviour of composite materials is typically non-linear [17]. Also under fatigue loading non-linear effects need to be considered, such as the influence of creep [18] and other dissipative mechanisms as viscoelasticity, viscoplasticity and damage growth. These effects can be investigated from the analysis of mechanical parameters during the fatigue test.

Four test samples are analysed in detail here to demonstrate the effects. Two samples in the range of intermediate lives: the dry sample that failed at 29 416 cycles and the conditioned sample that failed at 29 229 cycles; and two samples reaching the longest lives: the dry sample that failed at 1 495 222 cycles and the conditioned sample that failed at 686 118 cycles.

Fig.6 shows the evolution of the dynamic secant modulus for the intermediate lives (a) and for the long lives (b). It is possible to observe in both cases a clear and steady decrease in

modulus from the beginning of the test for the conditioned samples, while for the dry samples this strong decrease is limited until the final stage of the test ($N/N_f > 90\%$).

Fig. 6. Normalized dynamic secant modulus for dry and conditioned intermediate lives (a) and long lives (b). The results are normalized with respect to the dry secant modulus.

Figs. 7-8 show the hysteresis loops at 1, 25, 50, 75 and 99% of the number of cycles to failure of the dry and conditioned samples. **Fig. 7** reports the results for intermediate lives while **Fig. 8** reports the results for long lives.

Fig. 7. Normalized hysteresis loops at 1%, 25 %, 50 %, 75 % and 99 % of the fatigue life of (a) dry and (b) conditioned sample failed at intermediate fatigue lives (29416 cycles and 29229 cycles respectively). The results are normalized with respect to the dry ultimate strength.

Fig. 8. Normalized hysteresis loops at 1%, 25 %, 50 %, 75 % and 99 % of the fatigue life of (a) dry and (b) conditioned sample failed at long fatigue lives (1495222 cycles and 686118 cycles respectively). The results are normalized with respect to the dry ultimate strength.

From the hysteresis loops it is possible to observe that dry samples, **Figs. 7(a)** and **8(a)**, maintain a quite constant slope of the stress strain curve, associated with a constant dynamic secant modulus. Similarly, a limited increase of area is observed inside the hysteresis loop, associated with dissipated energy. The main change that was visible from the hysteresis loops of dry samples was the shifting of the hysteresis loops toward greater deflections, associated with creep effects.

Conditioned samples, **Figs. 7(b)** and **8(b)**, also presented a shift of the hysteresis loops toward greater deflections, but it was also possible to observe a decrease in slope, associated with a decrease of the dynamic secant modulus and a strong increase in the areas inside the hysteresis loop, associated with an increase of the cyclic dissipated energy. The observations were consistent for both intermediate lives, **Fig. 7**, and long lives, **Fig.8**.

In order to further analyse the effect of creep, the minimum cyclic deflection was analysed [18], defined as the deflection corresponding to the minimum load during the cycle, **Figs. 9 (a)** for intermediate fatigue lives and **9 (b)** for long fatigue lives.

Fig. 9. Deflection at the minimum of the cycle for dry and conditioned samples: (a) intermediate fatigue lives, (b) long fatigue lives.

It was possible to notice that both dry and conditioned samples showed an increase in minimum cyclic deflection with an increase of number of cycles, which was greater for conditioned samples. The behaviour was consistent for intermediate fatigue lives, **Fig. 9 (a)**, and long fatigue lives, **Fig. 9 (b)**.

Another parameter of interest for understanding the behaviour of the material during fatigue loading is the cyclic hysteresis dissipated energy, defined as the area inside a hysteresis cycle [19], **Figs. 10 (a)** for intermediate lives and **10 (b)** for long lives.

Fig. 10. Hysteresis dissipated energy: (a) intermediate fatigue lives, (b) long fatigue lives.

It is possible to notice, for the conditioned samples, a stronger increase in hysteresis dissipated energy compared to the dry samples, which is associated to damage [18], viscoelastic and viscoplastic dissipated energy [19]. In this case, the sample tested to intermediate lives showed a steeper increase in hysteresis dissipated energy compared to the sample tested to long fatigue lives. A possible explanation for this difference is provided in the discussions paragraph.

3.4. Microscopy analysis and visual observations

Optical micrographs were performed on the tested samples to analyse the damage mechanism. For dry samples, cracks appeared consistently in the web of the I-beam samples in the resin rich area between adjacent plies: the *inter-ply*, as shown in **Fig. 11**.

For the conditioned samples, damage was observed in the form of cracks in the web of the I-beam, inside the ply: in the *intra-ply*. These cracks are shown in **Fig. 12**.

Fig. 11. Optical micrographs of dry samples cross section. Cracks develop in the resin rich area between two adjacent plies.

Fig. 12. Optical micrograph of conditioned samples cross section. Cracks develop inside the plies.

These observations were further confirmed by translucency pictures taken on tested samples, **Fig. 13**. It was possible to observe a localized damage concentrated in few spots for the dry samples, **Fig. 13 (a)**, consistent with an intra-ply crack, and a widespread damage in the conditioned samples, **Fig. 13 (b)**, consistent with inter-ply cracks.

Intuitively, this difference can be explained with the fact that dry samples develop cracks in the inter-ply areas, which are a small amount of the overall ply cross-section. Conditioned samples develop cracks inside the plies, which account for most of the cross-section of the specimen. This leads to cracks localized in few spots for the dry samples and more widely extended cracks for the conditioned samples.

Damage occurs in the web of the I-beam, in the area between the loading noses, which is the area where the highest shear stresses occur, as predicted by linear beam theory [12, 16, 20, 21].

Fig. 13. Picture of (a) dry and (b) conditioned tested samples. It is possible to observe a localized damage for the dry samples and a widely spread damage for the conditioned samples.

In order to understand whether hygrothermal swelling introduces damage in the sample, an additional sample was conditioned and analysed under a microscope without being

mechanically loaded. In the web of the sample it was possible to observe damage, in the form of fiber/matrix debondings, **Fig. 14 (a), (b)**. This damage was not observed in unconditioned samples. The debondings suggest that the conditioned samples are weakened even before the fatigue testing is started.

Fig. 14. Optical micrograph of conditioned untested sample. Fiber/matrix debondings are visible: (a) around a single fiber, (b) on two adjacent fibers.

4. Discussions

4.1 Overview

The experimental results are summarized in **Table 2**. Analysis of these parameters enables understanding the different fatigue damage mechanisms occurring for dry and conditioned samples.

Table 2. Summary of the experimental results for dry and conditioned samples.

For dry samples, **Fig. 9**, shows a constant increase of minimum deflection with increasing number of cycles. This behaviour can be caused by either creep in the matrix [22] or damage development. However, the second reason can be excluded, because **Figs. 6**, **10** show that dry samples do not show a strong decrease in dynamic secant modulus, nor a strong increase in hysteresis dissipated energy, both parameters associated to damage development or growth [18, 23]. The influence of matrix creep on the fatigue behaviour of dry samples is also consistent with the microscopy analysis of tested samples. In fact, in **Fig. 11**, cracks were found on the inter-ply, a resin rich area.

4.2 Damage development in dry samples

The fatigue degradation mechanism for dry samples is schematized in **Fig. 15 (a)**. Under mechanical cycling loading creep occurs, which is concentrated in the inter-ply, the resin rich region between neighbouring plies, and finally failure occurs in the border between the ply and the resin rich inter-ply, as shown in **Fig.11**.

Fig. 15. Schematized fatigue degradation mechanism for (a) dry and (b) conditioned samples.

For conditioned samples, it is possible to observe a steady increase in cyclic minimum deflection similarly to the dry samples, **Fig. 9**, but also a decrease in secant dynamic modulus, **Fig. 6**, and an increase in hysteresis dissipated energy, **Fig. 10**, which was less pronounced in the dry samples.

These observations suggest that while the fatigue failure mechanism of the dry samples was creep dominated, the fatigue failure mechanism of the conditioned samples was dominated by growth of initial damage. This mechanism explains the steady increase of hysteresis dissipated energy and decrease of dynamic secant modulus during the tests.

The microscopy analysis on tested samples shows that for conditioned samples, **Fig. 12**, cracks appear within the ply: in the intra-ply, differently from the dry case, where cracks appear in the inter-ply. This suggests that the damage occurs in an area where the highest stress concentrations are present, where the fibers closely packed together.

The damage mechanism that influences the fatigue behaviour of conditioned samples is believed to be the hygrothermal induced fiber/matrix debonding, which was observed in unloaded conditioned samples by means of microscopy analysis in **Fig. 14** and has been reported in other studies too [12, 24, 25].

4.3 Damage development in conditioned samples

The fatigue degradation mechanism for conditioned samples is schematized in **Fig. 15 (b)**, where prior to loading, damage is already present in the form of fiber/matrix debondings, as shown in **Fig. 14**. Under loading microcracks develop from the debondings and the final failure is caused by cracks developing in the intra-ply, as shown in **Fig. 12**.

In **Fig. 10**, it was observed that hysteresis dissipated energy during the fatigue test of the conditioned samples showed a different behaviour for the intermediate and long lives. The main difference between the two cases is the magnitude of cyclic load, hence stress, applied to the samples. For intermediate lives, the cyclic stress applied on the sample is believed to be above the threshold value that causes a steady growth of crack starting from the fiber/matrix debondings. For the long fatigue lives, lower stresses are applied to the sample, which are believed to be below the threshold value that causes steady crack growth from the fiber/matrix debondings. For the samples tested in the intermediate lives, with loads below the crack growth threshold it was still possible to observe a decrease of dynamic secant modulus, **Fig. 6**, and an increase of minimum cyclic deflection, **Fig.9**, which imply that another cyclic degradation mechanism is taking place which is not likely to be matrix creep, as this would not lead to a decrease in secant dynamic modulus. It is believed that this effect could be attributed to a moisture induced fiber/matrix interface degradation.

Finally, a limitation of the test method proposed here needs to be discussed. For any sample geometry, intermediate states are usually hard to test experimentally, due to the non-uniform concentration profile inside the sample. The I-beam specimens, due to their complex shape, are recommended when comparing dry and saturated conditions, but not when studying intermediate conditions, as gradients of fluid concentration in the material would be expected in that case, between web and flanges.

5. Conclusions

Interlaminar shear fatigue of composites was studied in this work using a novel test method, the I-beam short beam shear test. This test method is similar to the standard short beam shear, the main difference is the I-shaped cross section of the specimen, which accelerates fluid saturation and the use of a four-point bending configuration which reduces the rollers indentation. The limitations of the test method are the complex shape of the specimens, compared to the traditional SBS configuration and the fact that the test is indicated for a comparison of dry and saturated conditions, while for intermediate conditions the non-uniform fluid concentration inside the material could influence the results. The acceleration of fluid saturation is further promoted by conditioning the samples at high temperature, 60°C, and then testing them at room temperature. It should be noted that upon saturation the glass transition temperature of the material decreased below the conditioning temperature. However the used for specimens were later tested at room temperature, and is therefore believed that this effect didn't influence the mechanical behaviour of the material.

Mechanical parameters were recorded during the test and analysed, in order to investigate the evolution of deflection, stiffness and hysteresis dissipated energy during the test. Microscopy analysis on dry and conditioned tested samples were performed along with untested reference samples, both dry and conditioned.

It was possible to observe a strong decrease of fatigue life for conditioned samples and a change in slope of the SN curve, attributed to a change of the failure mode.

The failure mode observed for dry samples was initial creep localized in the resin rich inter-ply finally developing into a crack in the interlaminar region, **Fig. 15 (a)**.

For the conditioned samples damage started prior to loading due to hygrothermal swelling in the form of fiber/matrix debonding. Upon loading damage developed as microcracks inside the ply (intra-ply) and finally developed into cracks in the intra-ply region.

The change in failure mode observed here can be used for the development of models for the analysis and prediction of interlaminar shear fatigue behaviour of dry and conditioned composites, taking into account the different failure mechanisms that can occur in both cases. The findings suggest that fiber/matrix interface plays a crucial role in the interlaminar shear fatigue performance of conditioned glass fiber/epoxy composites, and the immersed fatigue behaviour of the material can be improved by increasing the resistance of the interface.

Acknowledgements

This work is part of the DNV GL led Joint Industry Project "Affordable Composites" with nine industrial partners and the Norwegian University of Science and Technology (NTNU). The authors would like to express their thanks for the financial support by The Research Council of Norway (Project 245606/E30 in the Petromaks 2 programme).

The authors would like to thank also Carl-Magnus Midtbø and Børge Holen for designing and manufacturing an immersion testing chamber.

Declaration of interest

None

References

1. Mejri, M., et al., *Hygrothermal aging effects on mechanical and fatigue behaviors of a short- natural-fiber-reinforced composite.* International Journal of Fatigue, 2018. **108**: p. 96-108.
2. Mortazavian, S. and A. Fatemi, *Fatigue of short fiber thermoplastic composites: A review of recent experimental results and analysis.* International Journal of Fatigue, 2017. **102**: p. 171-183.
3. Mishnaevsky, L., et al., *Materials for Wind Turbine Blades: An Overview.* Materials (Basel), 2017. **10**(11).
4. Salama, M.M., et al., *The First Offshore Field Installation for a Composite Riser Joint*. Offshore Technology Conference.
5. Echtermeyer, A.T., *Integrating Durability in Marine Composite Certification*, in *Durability of Composites in a Marine Environment*, P. Davies, Rajapakse Yapa D.S., Editor. 2014, Springer Netherlands: Amsterdam. p. 179-194.

6. Schneider, K. and R.W. Lang. *Second source qualification of carbon fiber/epoxy prepregs for primary and secondary airbus structures*. in *Plastics, metals, ceramics : proceedings of the 11th International European Chapter Conference of Society for the Advancement of Material and Process Engineering*. 1990. Basel, Switzerland.
7. Baley, C., et al., *Application of Interlaminar Tests to Marine Composites. A Literature Review.* Applied Composite Materials, 2004. **11**(2): p. 99-126.
8. ASTM, *D2344/D2344M-16 Standard Test Method for Short-Beam Strength of Polymer Matrix Composite Materials and Their Laminates*. 2016, ASTM International: West Conshohocken, PA.
9. Rocha, I.B.C.M., et al., *Hygrothermal ageing behaviour of a glass/epoxy composite used in wind turbine blades.* Composite Structures, 2017. **174**(Supplement C): p. 110-122.
10. ASTM, *Standard Test Methods for Constituent Content of Composite Materials*. 2015, ASTM International, West Conshohocken, PA.
11. ASTM, *Standard Test Method for Moisture Absorption Properties and Equilibrium Conditioning of Polymer Matrix Composite Materials*. 2014, ASTM International, West Conshohocken, PA.
12. Gagani, A., Krauklis, A., Vedvik, N.-P., Echtermeyer, A. T., *Experimental study of interlaminar shear strength of glass fiber epoxy composites in humid environment. Methodology and results.* To appear, 2018.
13. Gagani, A., Fan Y., Muliana, A.H., Echtermeyer, A.T., *Micromechanical modeling of anisotropic water diffusion in glass fiber epoxy reinforced composites.* Journal of Composite Materials, 2017. **52**(17): p. 2321-2335.
14. Basquin, O.H., *The Exponential Law of Endurance Tests.* American Society for Testing and Materials Proceedings, 1910. **10**: p. 625-360.
15. Xie, M. and D.F. Adams, *A plasticity model for unidirectional composite materials and its applications in modeling composites testing.* Composites Science and Technology, 1995. **54**(1): p. 11-21.
16. He, Y. and A. Makeev, *Nonlinear shear behavior and interlaminar shear strength of unidirectional polymer matrix composites: A numerical study.* International Journal of Solids and Structures, 2014. **51**(6): p. 1263-1273.
17. Lubin, G., *Handbook of Composites*. 1 ed. 1982: Springer US.
18. Movahedi-Rad, A.V., T. Keller, and A.P. Vassilopoulos, *Fatigue damage in angle-ply GFRP laminates under tension-tension fatigue.* International Journal of Fatigue, 2018. **109**: p. 60-69.
19. Launay, A., et al., *Multiaxial fatigue models for short glass fibre reinforced polyamide. Part II: Fatigue life estimation.* International Journal of Fatigue, 2013. **47**: p. 390-406.
20. Rosselli, F. and M.H. Santare, *Comparison of the short beam shear (SBS) and interlaminar shear device (ISD) tests.* Composites Part A: Applied Science and Manufacturing, 1997. **28**(6): p. 587-594.
21. Pahr, D.H., et al., *A study of short-beam-shear and double-lap-shear specimens of glass fabric/epoxy composites.* Composites Part B: Engineering, 2002. **33**(2): p. 125-132.
22. de Vasconcellos, D.S., F. Touchard, and L. Chocinski-Arnault, *Tension–tension fatigue behaviour of woven hemp fibre reinforced epoxy composite: A multi-instrumented damage analysis.* International Journal of Fatigue, 2014. **59**: p. 159-169.
23. Petermann, J. and K. Schulte, *The effects of creep and fatigue stress ratio on the long-term behaviour of angle-ply CFRP.* Composite Structures, 2002. **57**(1): p. 205-210.

24. Weitsman, Y., *Coupled damage and moisture-transport in fiber-reinforced, polymeric composites.* International Journal of Solids and Structures, 1987. **23**(7): p. 1003-1025.
25. Weitsman, Y.J. and M. Elahi, *Effects of Fluids on the Deformation, Strength and Durability of Polymeric Composites – An Overview.* Mechanics of Time-Dependent Materials, 2000. **4**(2): p. 107-126.

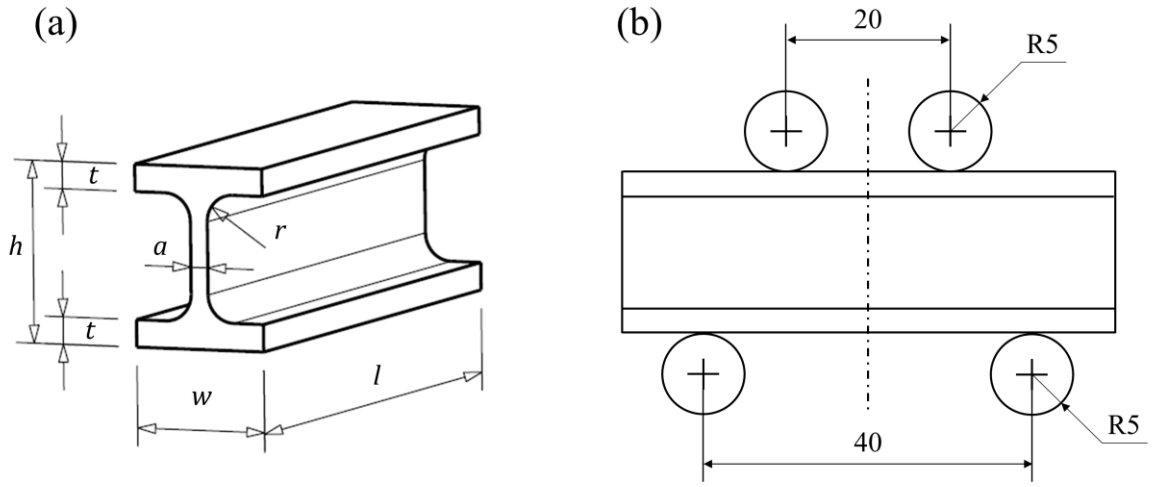

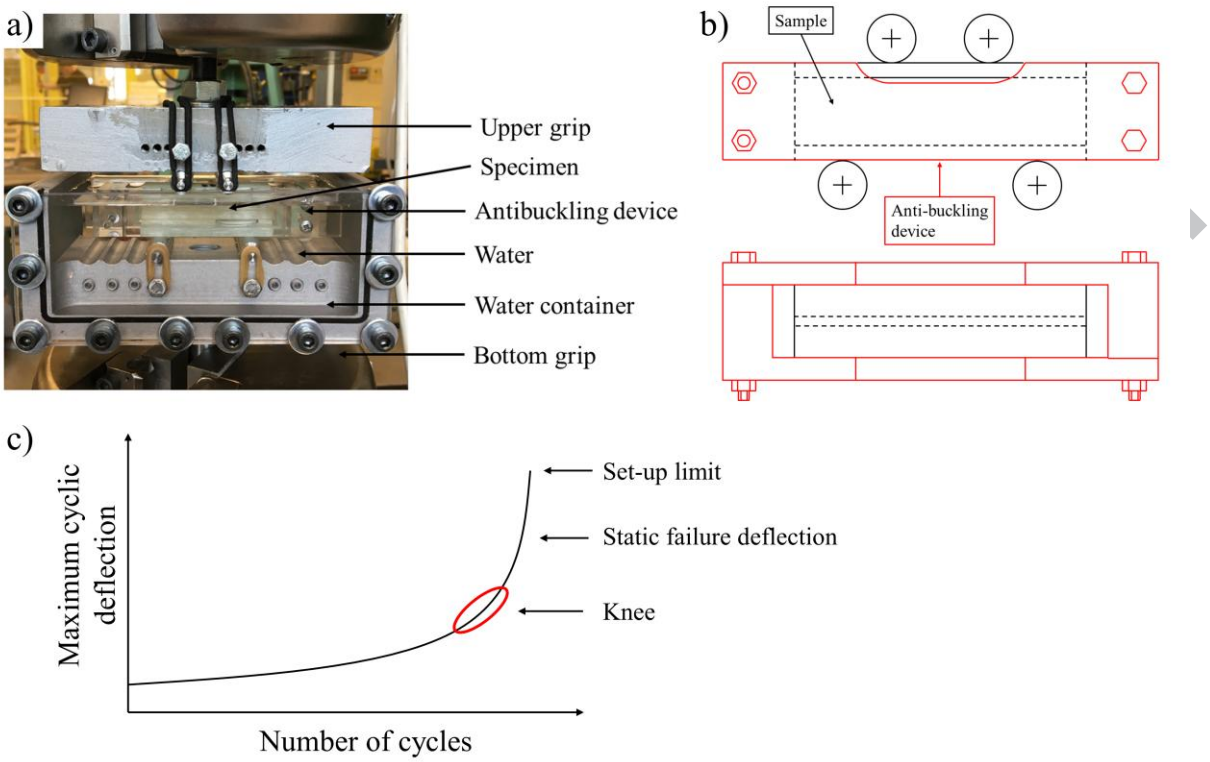

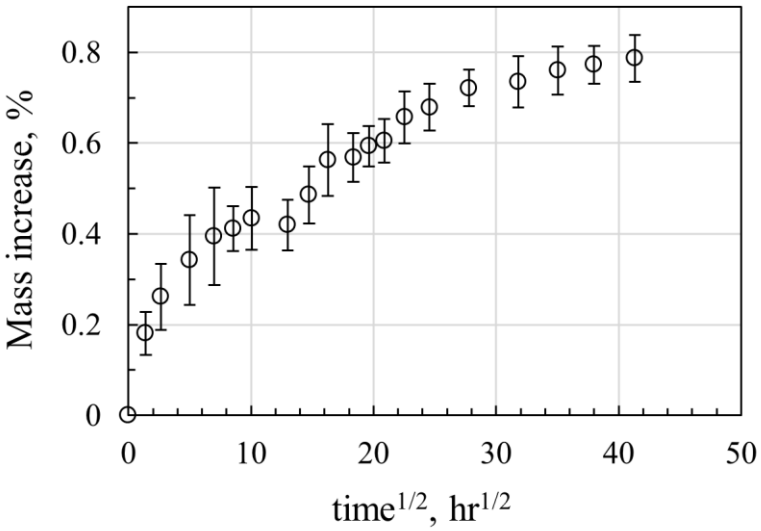

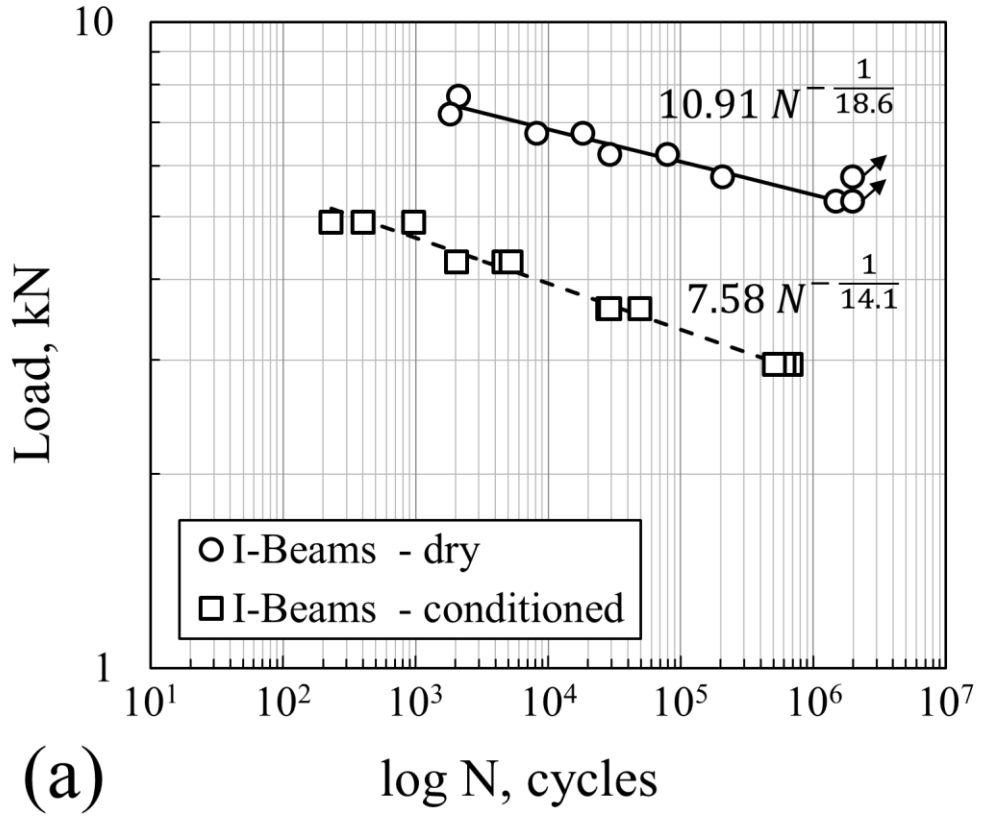

(a)

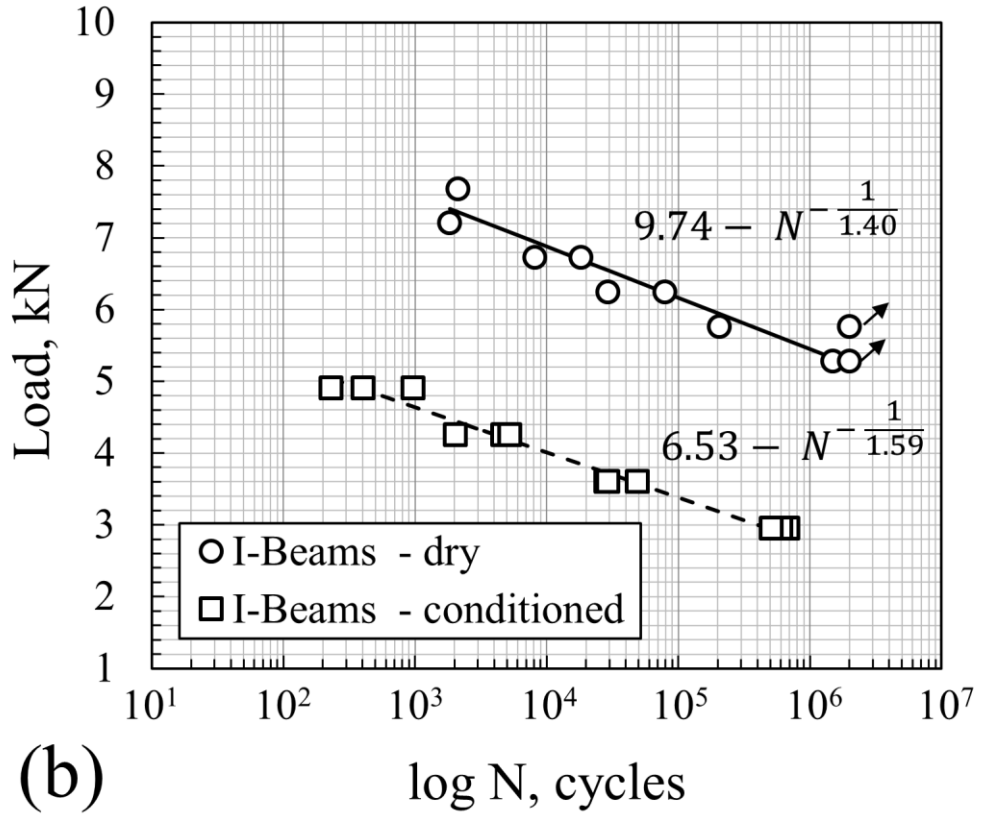

(b)

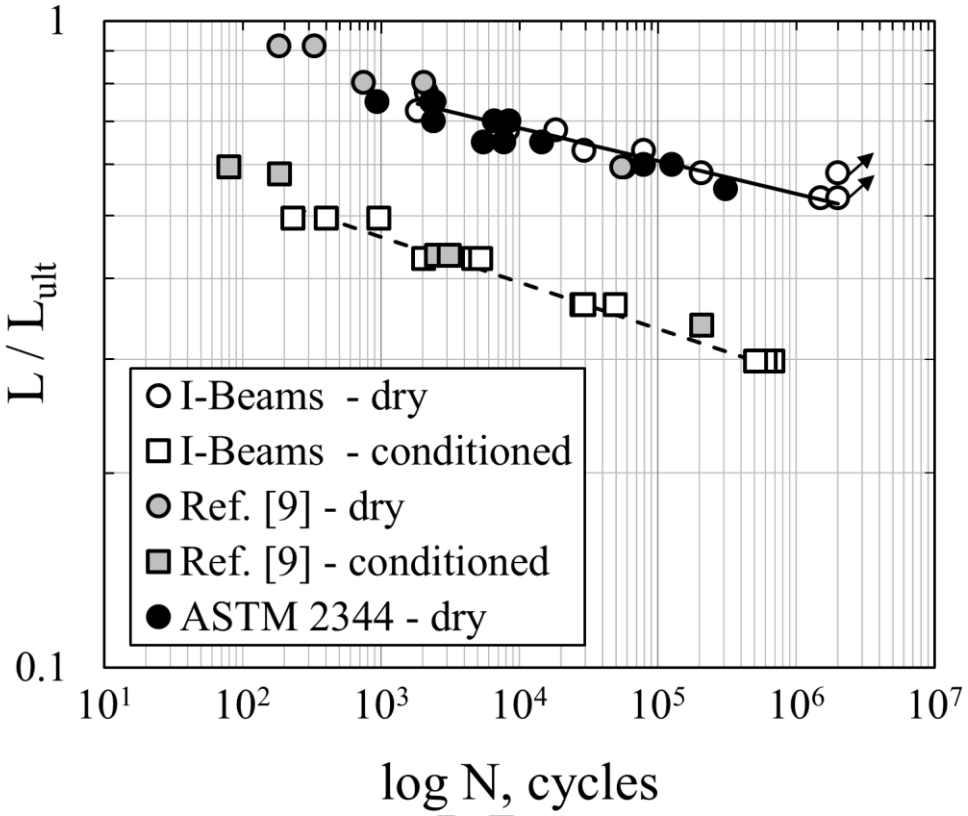

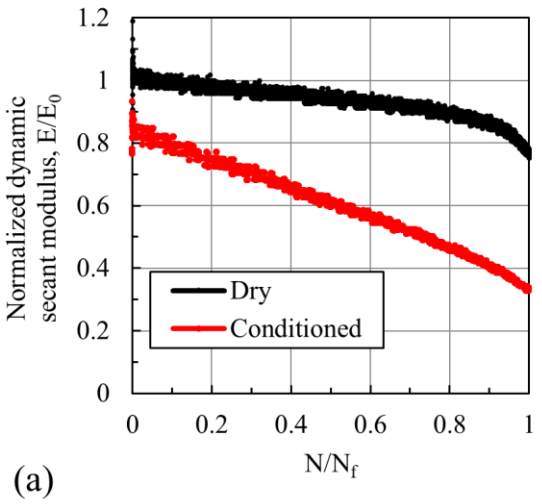

(a)

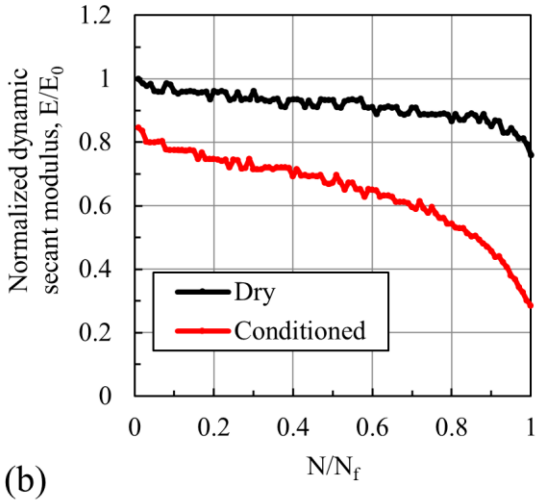

(b)

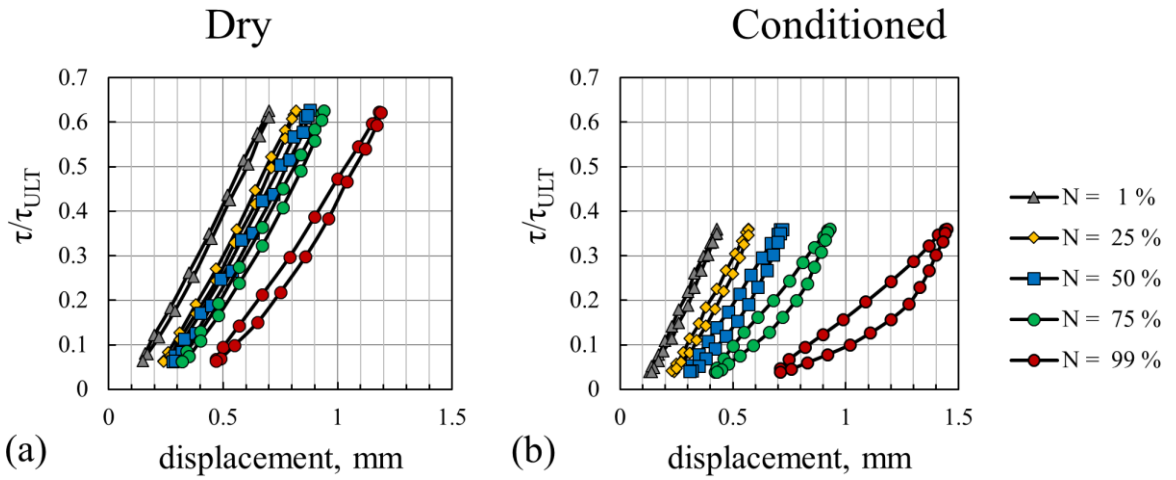

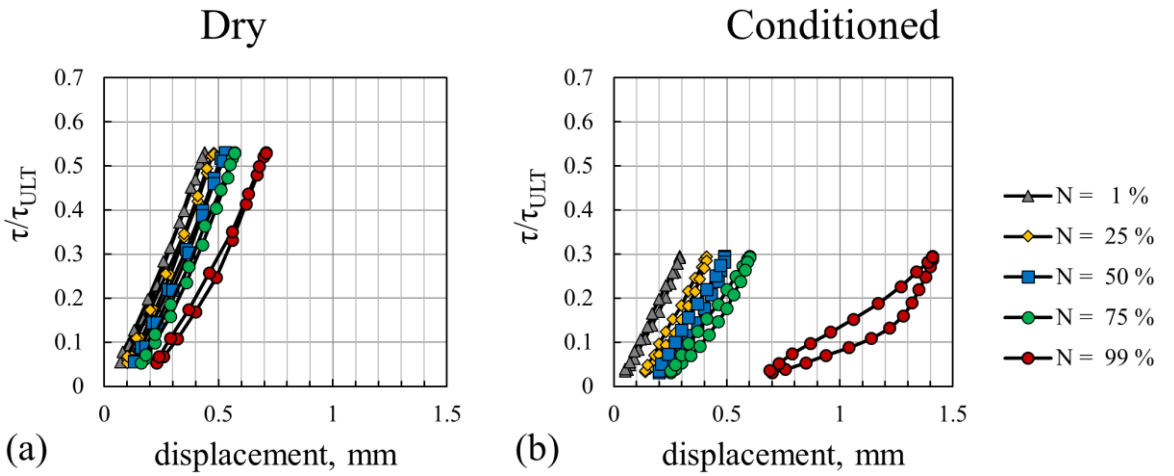

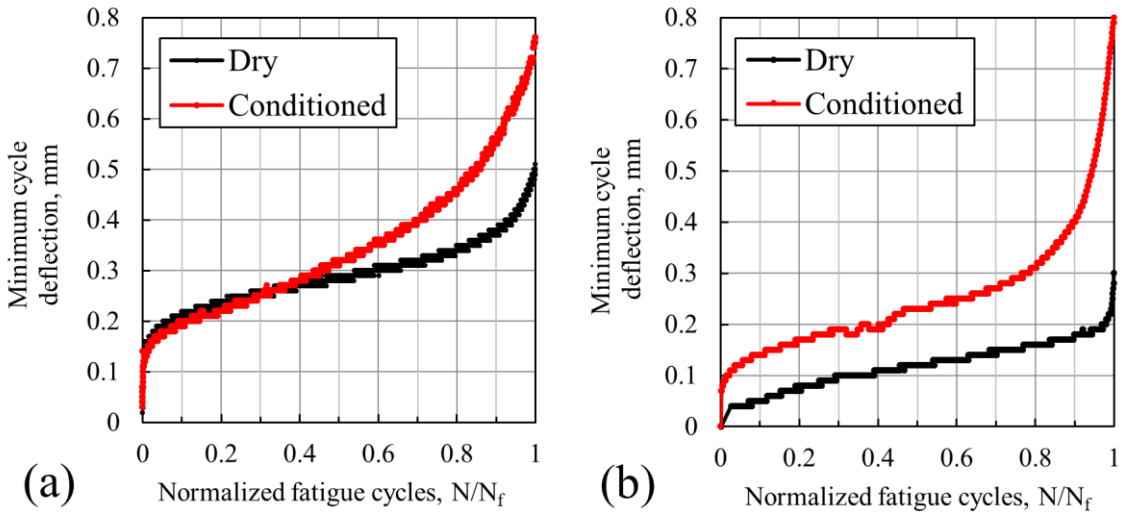

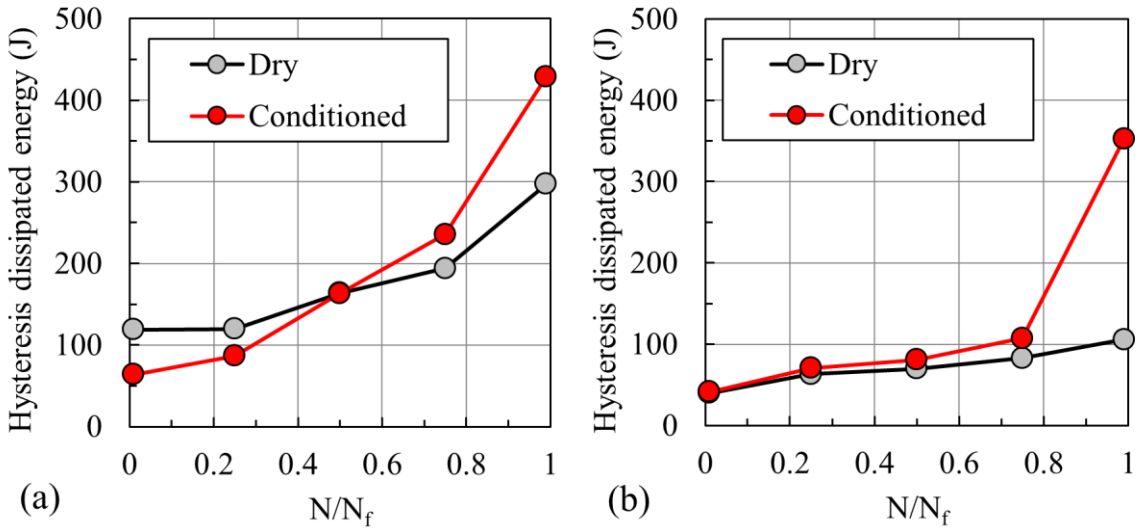

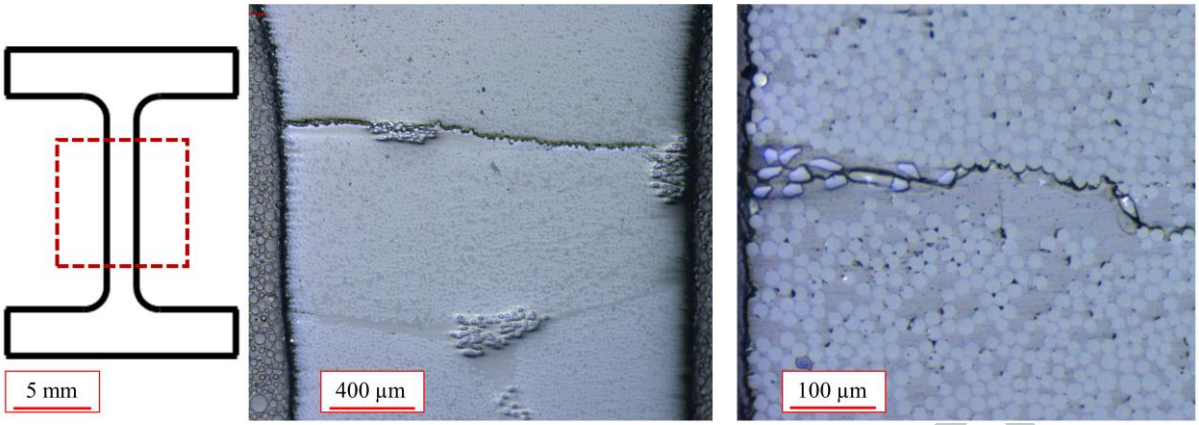

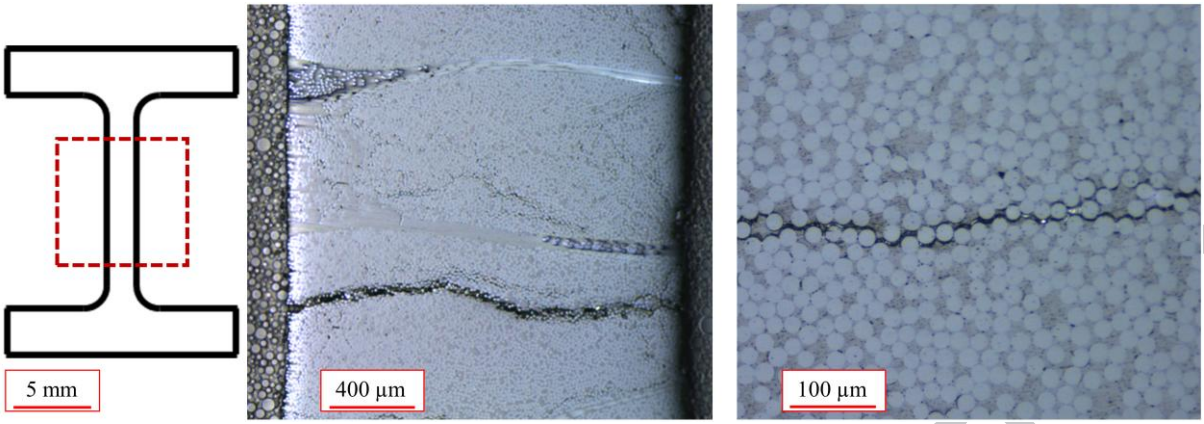

a) DRY

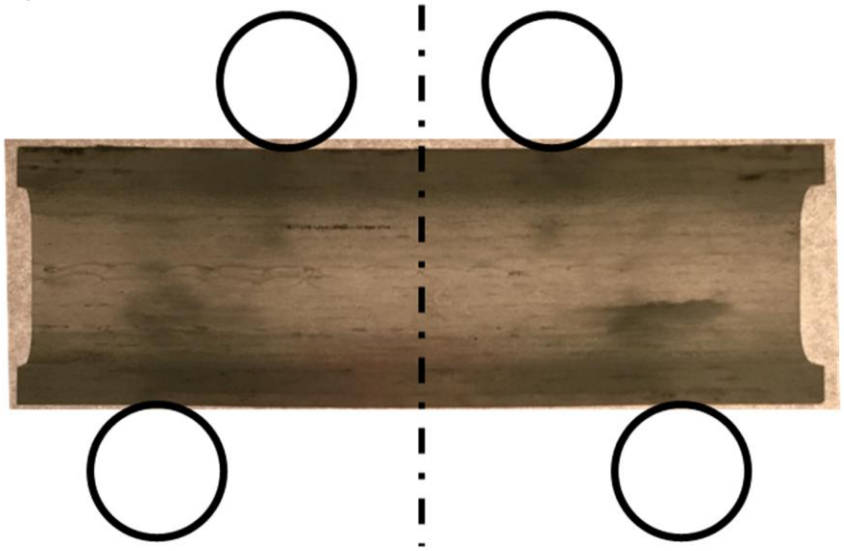

b) CONDITIONED

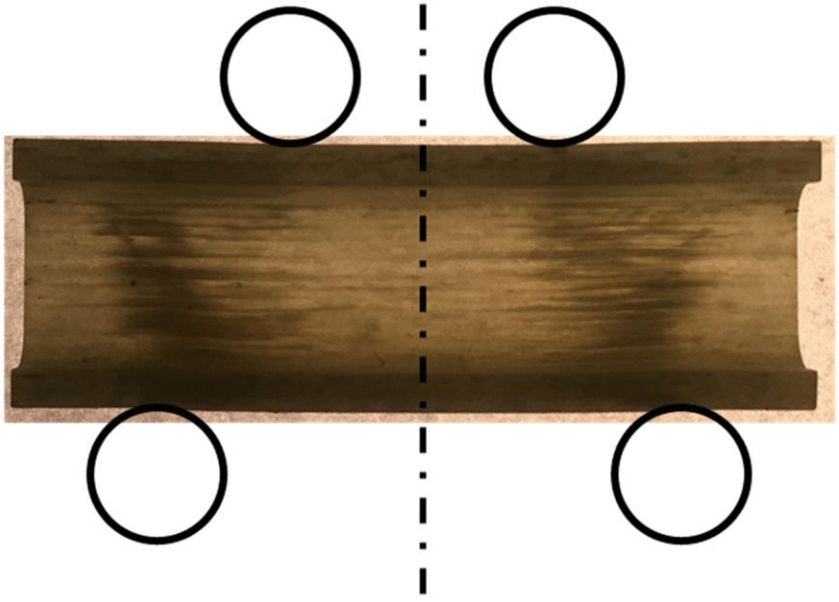

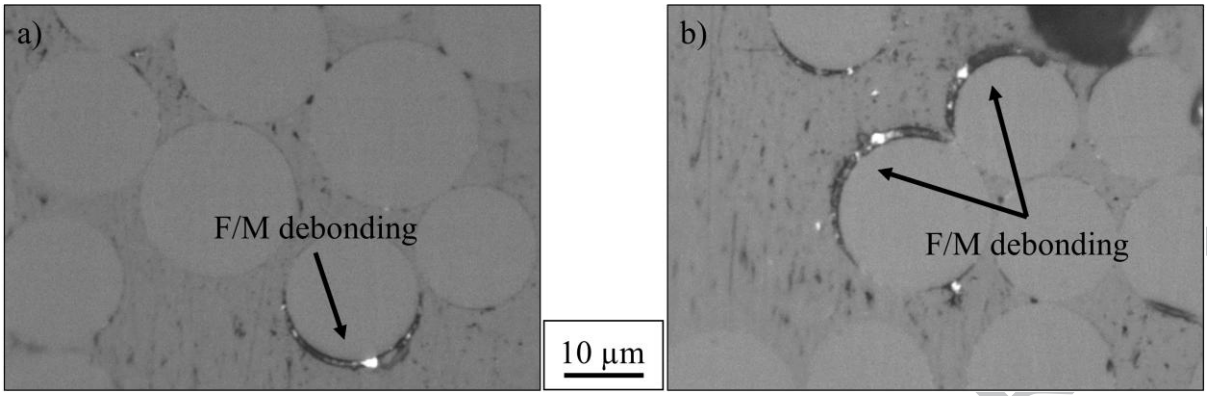

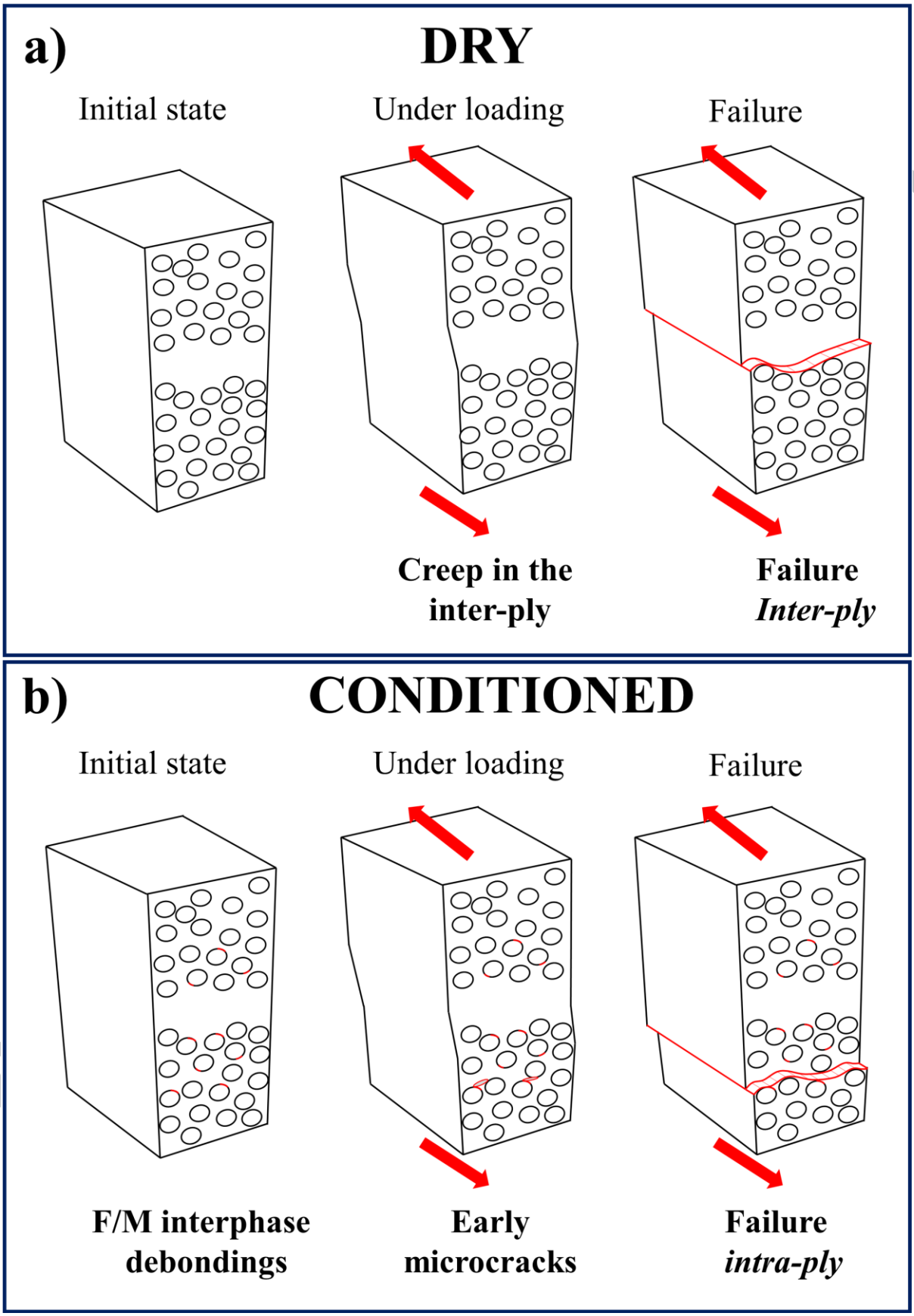

Tables

Table 1 Dimensions of the I-Beams specimen

Dimensions	w (mm)	l (mm)	h (mm)	t (mm)	a (mm)	r (mm)
	15	60	20	3	2	3

Table 2. Summary of the experimental results for dry and conditioned samples.

Parameter	**Dry**	**Conditioned**	**Shown in**
Optical microscopy	Inter-ply crack	Intra-ply crack	**Figs. 11-12**
Damage distribution	Localized	Spread	**Fig. 13**
Dynamic secant modulus	Steady, decreasing only towards end	Steady decrease during the entire test	**Fig. 6**
Hysteresis dissipated energy	Limited increase during the test	Steady increase during the entire test	**Fig. 10**
Minimum cyclic deflection at minimum loading in each cycle	Steady increase during the entire test	Steady increase during the entire test	**Fig. 9**
Presence of initial damage before fatigue testing	None	Yes, fiber/matrix debonding	**Fig. 14**

Highlights

- A novel test method for accelerated interlaminar shear fatigue of marine composites
- Comparison of dry and immersed interlaminar fatigue shear testing
- Matrix creep induced fatigue damage in dry samples
- Cracks growth induced fatigue damage in immersed samples